The determination of ionic transport properties at high pressures in a diamond anvil cell

Qinglin Wang,[1,2,3] Cailong Liu,[1] Yonghao Han,[1] Chunxiao Gao,[1,a)] and Yanzhang Ma[2,4,a)]
[1]*State Key Laboratory of Superhard Materials, Jilin University, Changchun 130012, China*
[2]*Center for High Pressure Science and Technology Advanced Research, Changchun 130012, China*
[3]*Shandong Key Laboratory of Optical Communication Science and Technology, School of Physical Science and Information Technology of Liaocheng University, Liaocheng 252059, China*
[4]*Department of Mechanical Engineering, Texas Tech University, Lubbock, Texas 79409, USA*

HPSTAR
325-2016

A two-electrode configuration was adopted in an *in situ* impedance measurement system to determine the ionic conductivity at high pressures in a diamond anvil cell. In the experimental measurements, Mo thin-films were specifically coated on tops of the diamond anvils to serve as a pair of capacitance-like electrodes for impedance spectrum measurements. In the spectrum analysis, a Warburg impedance element was introduced into the equivalent circuit to reveal the ionic transport property among other physical properties of a material at high pressures. Using this method, we were able to determine the ionic transport character including the ionic conductivity and the diffusion coefficient of a sodium azide solid to 40 GPa. *Published by AIP Publishing.* [http://dx.doi.org/10.1063/1.4971304]

I. INTRODUCTION

Unlike the studies of the electronic transportation that have been mainly focused on crystalline solids such as metals and semiconductors, the ionic transport studies are mainly performed in aqueous or organic salt solutions. Yet there are cases, such as in the application of solid electrolyte, where the dominant charge transportation by the ion itself as well as by both ion and minimal electron becomes crucial. At ambient conditions, impedance spectrum measurement method has long been conventional in the studies of electrical charge transportation and related physical properties.[1–5] Specially, using the impedance method, the presence of independent pathways for charge transportation in an inorganic material,[6] and the mixed electronic and ionic conduction in various organic and inorganic materials has been satisfactorily addressed.[7–11] The accurate determination of the impedance spectrum of a material under high pressure has only been recently achieved by introducing the fabrication of a micro-electrical circuit on the anvils in a diamond anvil cell.[12–15] Such a method provides a mean to introduce accurate impedance measurement in DACs under ultrahigh pressure and thus allows the investigation of grain boundary effect, as well as the dielectric and relaxation properties of materials.

The high-pressure impedance measurement system has been successful in resolving the electronic conductivity of many types of materials along with the physics behind them.[16–19] However, the study of the ionic conduction behavior of a material under high pressure has scarcely been tackled thus far due to the difficulties of the measurement itself and its subsequent data analysis. Most high-pressure ionic conductivity measurements were conducted with multi-anvils[20,21] or other apparatus,[22–25] which limited the pressure (<10 GPa). To investigate the ionic conductivity at much higher pressure, the measurement should be introduced to DAC. On the one hand, the electrodes in DAC should be designed and have a fixed position and regular geometrical shape. On the other hand, the insulation of the inside wall of the gasket hole should be fully considered, since even a small part of an electric short between sample and inside wall of the gasket could cause a large error during electrical measurement in DAC under high pressure.[26] For impedance measurement, this risk would be enhanced and then result in a large parasite impedance to the system. In the present work, we developed a flexible method for the determination of the ionic conductivity of a material *in situ* at high pressures. Using this method, we were able to confirm the ionic conductivity and determine its diffusivity of sodium azide to 40 GPa. Through such a routine method, one may expect to conveniently explore the transport behavior of ionic materials to high pressures upto 100 GPa level.

II. AC IMPEDANCE SPECTRUM MEASUREMENTS

The first process was to fabricate a pair of electrodes on top of the two diamond anvils used for pressure generation. A 0.3-μm-thick Mo film was sputtered on the diamond facets while the anvil was being heated at 600 K. The film was then shaped into a circular electrode of 170 μm in diameter by a photolithography and chemical etching process. After the pair of anvils was aligned in a diamond anvil cell, the two coated Mo films served as parallel-plate capacitor like electrodes in impedance measurements. The second process was the protection and insulation of the electrodes from contacting the conducting gasket. In this process, a 2-μm-thick alumina film was sputtered on top of the whole anvils including the formed electrodes in the first process. To allow the electrode contact the sample, the central area of the Al_2O_3 film was removed by a chemical method. The third process was the fabrication of a gasket. A sheet of T301 stainless steel was pre-indented to a thickness of

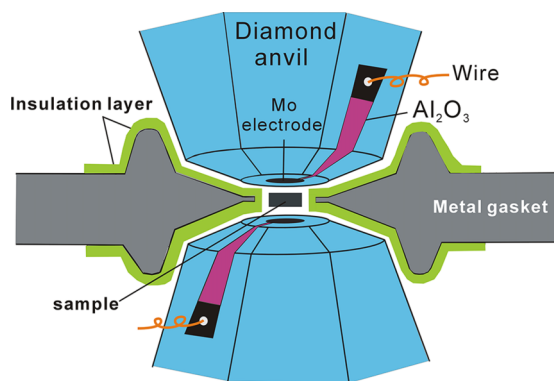a)Authors to whom correspondence should be addressed. Electronic addresses: cc060109@qq.com and y.ma@ttu.edu

FIG. 1. The cross section of the designed DAC device.

FIG. 2. 3D impedance of sodium azide at 15.3 GPa.

40 μm and a hole of 250 μm diameter was drilled. A fine Al_2O_3 powder mixed with minimal amount of epoxy was filled in the predrilled gasket hole that served as part of the sample chamber. After compacting enough powder into the hole, a smaller hole was drilled in the center of the compacted Al_2O_3, leaving a thin wall of Al_2O_3 between the metal wall and the new hole, which can prevent electrical conduction between the sample and the gasket. The schematic diagram of the designed DAC device is shown in Fig. 1.

In order to make accurate impedance measurement, the parasite capacitance and inductance have been tested before the measurement. It was found that the impedance of the sample chamber and the connecting wires reached a magnitude of about 10^{12} Ω and 10 Ω, respectively, which proved that the impedance coming from sample chamber and connecting wires has little influence on the impedance measurement.

In the test, a sodium azide sample was loaded into the sample chamber for measurements. The pressure was determined by ruby fluorescence method.[27] In the sample thickness measurements, the deformation of the diamond was considered to be elastic and the same at a given pressure during loading and unloading. Based on the assumption of completely plastic deformation on the gasket, the actual thickness of the sample (t) at every pressure during the compressing process can be expressed by $t = L_m + \delta_P$, where L_m represents the sample thickness at maximum pressure and δ_P is the thickness difference between loading and unloading at every pressure.[28] Impedance spectroscopy measurements were conducted using a Solartron 1260 impedance analyzer equipped with a Solartron 1296 dielectric interface. A 0.1 V sine signal was applied to the sample in the frequency range from 1 to 10^7 Hz.

III. IMPEDANCE SPECTRUM ANALYSIS

A. An equivalent-circuit

Fig. 2 illustrates a 3-D-perspective plot of the impedance of sodium azide at 15.3 GPa. The black line is the 3-D curve and its three 2-D projections are shown in the appropriate planes. The projection to the Z'', Z' plane is the conventional impedance-plane plot. The complex impedance spectra consist of two parts: a semicircle in high-frequency region and a straight line with a slope of 45° at low frequencies.
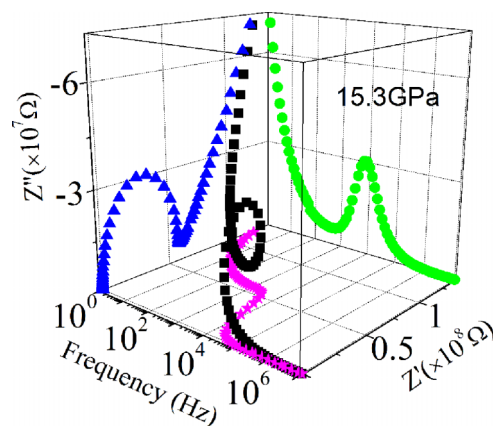
It is often useful to interpret impedance spectroscopy by the use of equivalent circuits. For an ideal Debye circuit (inset of Fig. 3), the ions are completely blocked at the sample/electrode interfaces and cannot diffuse through the sample. At low frequencies, no electrical current flows through the geometric capacitance due to its small value, which causes large impedance and leads to a characteristic series R-C configuration in the Nyquist plot. At high frequencies, electrical current can move through the geometric capacitance and the Nyquist plot shows a characteristic parallel R-C configuration. The corresponding Nyquist impedance plot of an ideal Debye circuit includes a semicircle in the high-frequency region and a straight line perpendicular to the x-axis in the low-frequency region.

The impedance spectra of the sodium azide sample deviate from the ideal Debye circuit spectrum. The plot gives a semicircle in the high-frequency region but a straight line with a slope of 45° in the low-frequency region. It has been shown that the deviation from ideal Debye circuit behavior relates to processes that occur at the sample/electrode interface.[29] A slope of 45° in the low-frequency region indicates that the charge carrier is not blocked at the sample/electrode interface, but diffuses into and out of the electrodes. This involves the introduction of a Warburg impedance into the equivalent
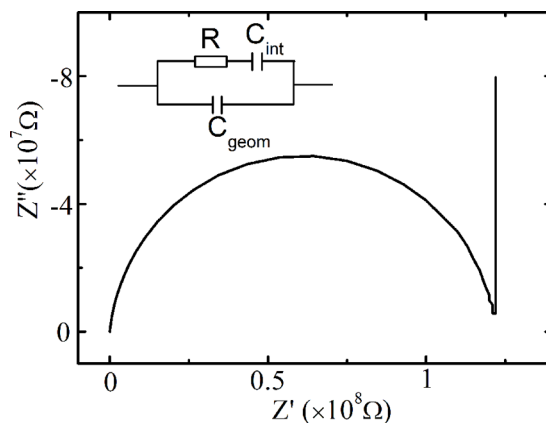

FIG. 3. The Nyquist plot corresponding to the ideal Debye equivalent circuit (the inset). R is the sample resistance and C_{int} is the capacitance formed by the two sample-electrode interfaces. C_{geom} is the geometrical capacitance formed by the two parallel metallic electrodes that sandwiched the sample.
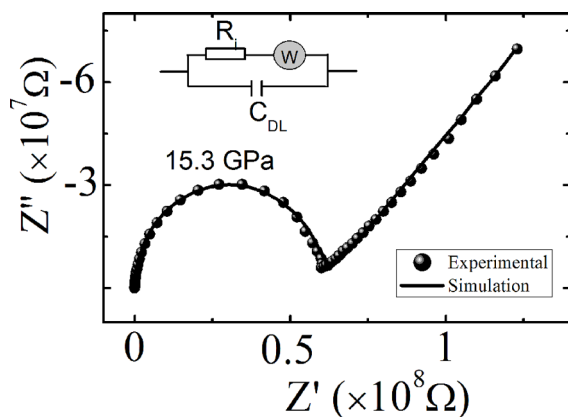
FIG. 4. The Nyquist-diagram at 15.3 GPa (data points). The continuous lines represent the simulated spectra. Inset is the circuit diagram equivalent to the conduction mechanism. R_i is the ionic transfer resistance, C_{DL} is the double-layer capacitance between the sample-electrode interfaces, W denotes the Warburg impedance. The parameter values are $R_i = 5.9 \times 10^7$ Ω, $C_{DL} = 4.3 \times 10^{-10}$ F, $W_T = 6.0 \times 10^{-12}$ Ω^{-1} S$^{0.5}$, $W_P = 0.265$, respectively.

circuit (Fig. 4). The Warburg impedance Z_ω satisfies[30]

$$Z_\omega = \sigma\omega^{-1/2} - j\sigma\omega^{-1/2}, \qquad (1)$$

where σ is the Warburg coefficient and ω is the angular frequency. Therefore, the transportation impedance in the system being studied has two parts: the ionic transfer resistance R_{ct} and the Warburg impedance Z_w between sample/electrode diffusion layers. The agreement between the simulated spectra and the experimental data indicates that the equivalent circuit describing the electrical response process in the sample is satisfactory.

B. Determination of the diffusion coefficient

In the process of ionic conduction, the relationship between Z' and $\omega^{-1/2}$ in the low-frequency region satisfies the following equation:[30]

$$Z' = Z_0' + \sigma\omega^{-1/2}, \qquad (2)$$

where Z_0' is a parameter independent of frequency, σ is the Warburg coefficient, and ω is the angular frequency. According to Eq. (2), the Warburg coefficient is acquired from the slope of
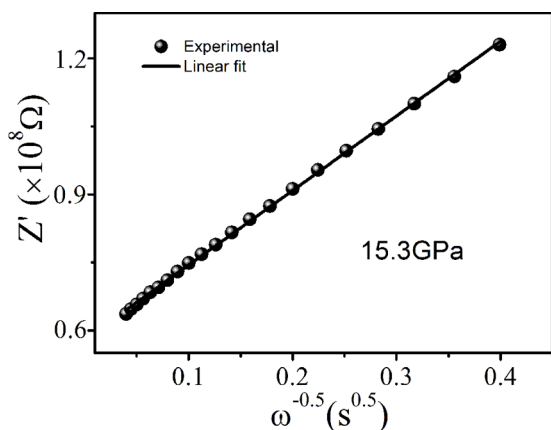

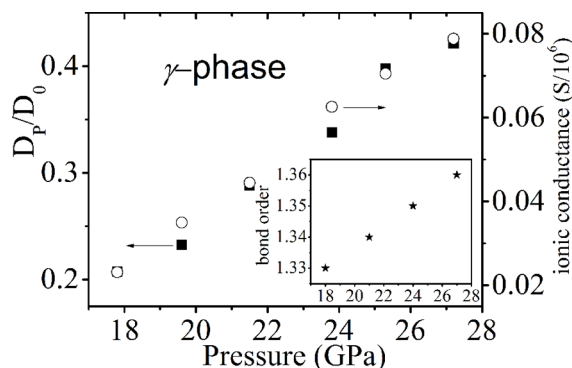FIG. 5. Z' vs $\omega^{-1/2}$ plot at low frequencies at 15.3 GPa.

FIG. 6. Pressure dependence of the diffusion coefficient and the ionic conductance in the γ-phase of sodium azide. Inset: the calculated bond order of the end N-central N bond in the azide anion in the γ-phase at different pressures.

Z'-$\omega^{-1/2}$ curves (as shown in Fig. 5). The diffusion coefficient of the ions (D_p) can be obtained from

$$D_P = 0.5(RT/AF^2\sigma C)^2, \qquad (3)$$

where R is the gas constant (8.314 J mol^{-1} K^{-1}), T is the temperature, A is the area of the electrode, F is Faraday's constant (96500 C mol^{-1}), and C is the molar concentration of cations. Let D_0 be the diffusion coefficient at the original pressure point and the D_p/D_0 under different pressures can be obtained.

C. Example: The ionic conduction in the *γ*-phase of a sodium azide

The parallel arrangement of azide ions in the γ-phase collapsed into a planar net and formed a T-like arrangement that is more favorable for linear azide during the α to γ phase transition, similar to that found in heavier azides.[31,32] The ionic diffusion coefficient increases with increasing pressure, and the ionic migration becomes easier in the γ-phase. The bond order of the end N-central N bond in the azide anion increases with increasing pressure (inset of Fig. 6), according to the calculation results, resulting in the increased intramolecular bonding strength in the azide anions. This leads to the increased interactions among nitrogen atoms in azide ions.

IV. CONCLUSION

A simple and convenient method has been developed to determine the ionic conduction behavior in a diamond anvil cell based on *in situ* impedance measurement. The ionic transport character of a sodium azide solid under high pressure was investigated using this method, where the bond order of the end N-central N bond in the azide anion increased with increasing pressure in the γ-phase, leading to the increased interactions among nitrogen atoms in azide ions. The developed method could provide a new means to study the ionic and ionic related properties of materials to a pressure attainable with a regular diamond anvil cell.

ACKNOWLEDGMENTS

[1]D. C. Sinclair and A. R. West, J. Appl. Phys. **66**, 3850 (1989).
[2]D. C. Sinclair, T. B. Adams, F. D. Morrison, and A. R. West, Appl. Phys. Lett. **80**, 2153 (2002).
[3]S. Dutta, R. N. P. Choudhary, P. K. Sinha, and A. K. Thakur, J. Appl. Phys. **96**, 1607 (2004).
[4]H. S. Hsu, J. C. A. Huang, S. F. Chen, and C. P. Liu, Appl. Phys. Lett. **90**, 102506 (2007).
[5]A. Dualeh, T. Moehl, N. Tétreault, J. Teuscher, P. Gao, M. K. Nazeeruddin, and M. Grätzel, ACS Nano **8**, 362 (2013).
[6]R. Huggins, Ionics **8**, 300 (2002).
[7]Y. Teraoka, H. Zhang, K. Okamoto, and N. Yamazoe, Mater. Res. Bull. **23**, 51 (1988).
[8]I. Riess, Solid State Ionics **44**, 207 (1991).
[9]I. Riess, Solid State Ionics **91**, 221 (1996).
[10]S. B. Adler, J. Lane, and B. Steele, J. Electrochem. Soc. **143**, 3554 (1996).
[11]I. Riess, Solid State Ionics **157**, 1 (2003).
[12]C. He, B. Liu, M. Li, and C. Gao, Rev. Sci. Instrum. **82**, 015104 (2011).
[13]Q. Wang, Y. Han, C. Liu, Y. Ma, W. Ren, and C. Gao, Appl. Phys. Lett. **100**, 172905 (2012).
[14]C. He, C. Gao, Y. Ma, M. Li, A. Hao, X. Huang, B. Liu, D. Zhang, C. Yu, G. Zou, Y. Li, H. Li, X. Li, and J. Liu, Appl. Phys. Lett. **91**, 092124 (2007).
[15]Y. Wang, Y. Han, C. Gao, Y. Ma, C. Liu, G. Peng, B. Wu, B. Liu, T. Hu, X. Cui, W. Ren, Y. Li, N. Su, H. Liu, and G. Zou, Rev. Sci. Instrum. **81**, 013904 (2010).
[16]W. Xin-Xin, H. Xiao-Ge, and B. Wu-Ming, Chin. J. Geophys. **59**, 624 (2016).
[17]N. Bagdassarov, J. Phys. Chem. Solids **72**, 236 (2011).
[18]K. Li, H. Y. Zheng, T. Hattori, A. Sano-Furukawa, C. A. Tulk, J. Moaison, M. Feygenson, I. N. Ivanov, W. Yang, and H. K. Mao, Inorg. Chem. **54**, 11276 (2015).
[19]L. Wang, F. Ke, Q. L. Wang, J. J. Yan, C. L. Liu, X. Z. Liu, Y. C. Li, Y. H. Han, Y. Z. Ma, and C. X. Gao, Appl. Phys. Lett. **107**, 201603 (2015).
[20]S. V. Goryainov, R. A. Secco, Y. Huang, and H. Liu, Physica B **390**, 356 (2007).
[21]S. V. Goryainov, R. A. Secco, Y. Huang, and A. Y. Likhacheva, Microporous Mesoporous Mater. **171**, 125 (2013).
[22]R. A. Secco, M. Rutter, and Y. Huang, Tech. Phys. **45**, 1447 (2000).
[23]O. Ohtaka, Y. Itakura, H. Arima, T. Kikegawa, and A. Yoshiasa, J. Phys. Soc. Jpn. **79**, 51 (2010).
[24]Z. Wojnarowska, A. Swiety-Pospiech, K. Grzybowska, L. Hawelek, M. Paluch, and K. L. Ngai, J. Chem. Phys. **136**, 164507 (2012).
[25]B. Sundqvist, M. G. Yao, and O. Andersson, High Pressure Res. **33**, 141 (2013).
[26]G. Peng, Y. H. Han, C. X. Gao, Y. Z. Ma, B. J. Wu, C. L. Liu, B. Liu, T. J. Hu, Y. Wang, X. Y. Cui, W. B. Ren, H. W. Liu, and G. T. Zou, Rev. Sci. Instrum. **81**, 036108 (2010).
[27]H. Mao, J.-A. Xu, and P. Bell, J. Geophys. Res. **91**, 4673, doi:10.1029/JB091iB05p04673 (1986).
[28]M. Li, C. X. Gao, G. Peng, C. Y. He, A. M. Hao, X. W. Huang, D. M. Zhang, C. L. Yu, Y. Z. Ma, and G. T. Zou, Rev. Sci. Instrum. **78**, 075106 (2007).
[29]I. Raistrick, C. Ho, and R. A. Huggins, J. Electrochem. Soc. **123**, 1469 (1976).
[30]C. Ho, I. D. Raistrick, and R. A. Huggins, J. Electrochem. Soc. **127**, 343 (1980).
[31]C. Choi and E. Prince, J. Chem. Phys. **64**, 4510 (1976).
[32]D. Hou, F. Zhang, C. Ji, T. Hannon, H. Zhu, J. Wu, V. I. Levitas, and Y. Ma, J. Appl. Phys. **110**, 023524 (2011).